AMERICAN SOCIETY FOR MICROBIOLOGY | Journal of Virology®

VIRUS-CELL INTERACTIONS

Membrane Interactions and Uncoating of Aichi Virus, a Picornavirus That Lacks a VP4

James T. Kelly,[a] Jessica Swanson,[a,b] Joseph Newman,[a] Elisabetta Groppelli,[c] Nicola J. Stonehouse,[b] Tobias J. Tuthill[a]

[a]The Pirbright Institute, Pirbright, United Kingdom
[b]School of Molecular and Cellular Biology, Faculty of Biological Sciences and Astbury Centre for Structural Molecular Biology, University of Leeds, Leeds, United Kingdom
[c]Institute for Infection and Immunity, St. George's University of London, London, United Kingdom

ABSTRACT Kobuviruses are an unusual and poorly characterized genus within the picornavirus family and can cause gastrointestinal enteric disease in humans, livestock, and pets. The human kobuvirus Aichi virus (AiV) can cause severe gastroenteritis and deaths in children below the age of 5 years; however, this is a very rare occurrence. During the assembly of most picornaviruses (e.g., poliovirus, rhinovirus, and foot-and-mouth disease virus), the capsid precursor protein VP0 is cleaved into VP4 and VP2. However, kobuviruses retain an uncleaved VP0. From studies with other picornaviruses, it is known that VP4 performs the essential function of pore formation in membranes, which facilitates transfer of the viral genome across the endosomal membrane and into the cytoplasm for replication. Here, we employ genome exposure and membrane interaction assays to demonstrate that pH plays a critical role in AiV uncoating and membrane interactions. We demonstrate that incubation at low pH alters the exposure of hydrophobic residues within the capsid, enhances genome exposure, and enhances permeabilization of model membranes. Furthermore, using peptides we demonstrate that the N terminus of VP0 mediates membrane pore formation in model membranes, indicating that this plays an analogous function to VP4.

IMPORTANCE To initiate infection, viruses must enter a host cell and deliver their genome into the appropriate location. The picornavirus family of small nonenveloped RNA viruses includes significant human and animal pathogens and is also a model to understand the process of cell entry. Most picornavirus capsids contain the internal protein VP4, generated from cleavage of a VP0 precursor. During entry, VP4 is released from the capsid. In enteroviruses this forms a membrane pore, which facilitates genome release into the cytoplasm. Due to high levels of sequence similarity, it is expected to play the same role for other picornaviruses. Some picornaviruses, such as Aichi virus, retain an intact VP0, and it is unknown how these viruses rearrange their capsids and induce membrane permeability in the absence of VP4. Here, we have used Aichi virus as a model VP0 virus to test for conservation of function between VP0 and VP4. This could enhance understanding of pore function and lead to development of novel therapeutic agents that block entry.

KEYWORDS Aichi virus, kobuvirus, picornavirus, VP4, VP0, uncoating, pore formation, viroporin, membranes

For many nonenveloped viruses, replication depends on the capsid first binding a receptor to trigger uptake into a cell via endocytosis. During entry the virus must deliver its RNA genome into the cytoplasm. Mechanisms of delivery are not well understood, but the proposed mechanism in picornaviruses (such as poliovirus [PV] and human rhinoviruses [RV]) involves capsid structural rearrangements that enable the virus to interact with the endosomal membrane and form a pore. The capsid then

Editor Anice C. Lowen, Emory University School of Medicine

Address correspondence to Tobias J. Tuthill, toby.tuthill@pirbright.ac.uk.

The authors declare no conflict of interest.

Received 13 January 2022
Accepted 31 January 2022
Published 16 March 2022

uncoats, releasing its genome through the pore, across the endosomal membrane, and into the cytoplasm. In many picornaviruses and picorna-like viruses, viral capsid protein VP4 is a small internal component of the capsid that is released during cell entry to initiate pore formation (1–7). VP4 is formed from the cleavage of capsid protein VP0 into VP2 and VP4 (8–10). However, certain picornaviruses do not undergo VP0 cleavage and therefore do not possess a VP4 protein, and it is unknown what component of the capsid performs the normal function of VP4.

The best-characterized picornavirus genera that possess uncleaved VP0 are kobuviruses and parechoviruses. Kobuviruses are associated with cases of acute gastroenteritis in people, livestock, and pets (11–14), including the best-studied member, the human pathogen Aichi virus (AiV). The virus is widespread, with 80% to 95% of adults reportedly having antibodies against the virus (15–17). AiV is generally asymptomatic; however, it can cause mild gastrointestinal upset and there have even been fatal cases reported in children under 5 years, especially in developing countries (14, 18–20).

Picornavirus particles consist of a single positive-sense RNA genome, within a nonenveloped capsid composed of 60 copies of four structural proteins, VP1, VP2, VP3, and VP4, arranged in pseudo-T=3 icosahedral symmetry. In the majority of picornaviruses, VP2 and VP4 are derived from a precursor called VP0, which undergoes a maturation cleavage to form VP2 and VP4 (e.g., enteroviruses, aphthoviruses, cardioviruses, and hepatoviruses); this is thought to be triggered by RNA encapsidation in some viruses (8–10, 21). However, for the kobuvirus and parechovirus genera, VP0 does not cleave and the mature capsid contains an intact VP0 (22, 23). In VP4-containing viruses, VP4 is usually myristoylated, and by using specific inhibitors or mutagenesis of a myristoylation signal sequence to prevent myristoylation, it has been shown to play a critical role in virus assembly and entry (24–27). The N terminus of kobuvirus VP0, but not parechovirus VP0, is myristoylated (22, 28); however, myristoylation seems unlikely to play an essential role as the specific inhibitors are unable to restrict infection by these viruses (28). Uncoating has been extensively studied in VP4-containing picornaviruses, especially enteroviruses (e.g., PV and RV). However, there are few studies on uncoating in VP0-containing viruses and no studies have been reported on the role of VP0 in uncoating, although it is assumed that the N terminus of VP0 may be involved in pore formation as this is in an analogous location to VP4.

In order to uncoat and form a pore within the endosomal membrane, viral capsids must undergo extensive structural rearrangements. Experimental and structural studies of different types of picornavirus particles have given great insights into the structural rearrangements that occur during uncoating of VP4-containing picornaviruses (29–37). The trigger varies between viruses: for aphthoviruses, these changes can be initiated solely by exposure to low pH (38, 39), while for major group RV, receptor interactions in combination with endosomal acidification are required (40–43). AiV capsids are known to be destabilized by low pH, and therefore, endosomal acidification may play a role in AiV uncoating (44).

Studies with enterovirus particles have shown that these viruses are able to bind to and permeabilize membranes, during a process known as capsid breathing (2, 45). Studies using intact virions, peptides of VP1-N and VP4, and antibodies raised against VP1-N and VP4, in conjunction with membrane binding and pore formation assays, revealed that the N terminus of VP1 is involved in attaching the enterovirus capsid to the membrane and VP4 is involved in pore formation (7, 45–47). We have shown previously that recombinant VP4 and VP4 peptides of rhinovirus 16 (RV16) form size-selective pores in model membranes consistent with the size of a single strand of RNA to allow it to pass through (2, 7). Furthermore, mutation of residue T28 in PV VP4 can reduce the capsid's ability to permeabilize model membranes (5). In combination with these biophysical data, structural studies have helped develop a model for enterovirus uncoating. Incubation of enterovirus particles with their receptor or heating past physiological temperature can trigger mature particles to uncoat into uncoating intermediate particles (altered particles [A-particles]) or empty particles (30). A-particles still

contain the viral genome, but the capsid has undergone expansion and structural rearrangements, including VP4 release and externalization of the N terminus of VP1, whereas empty particles have released their genome and undergone further structural rearrangements (29–37). Biophysical and structural data on PV in the presence of model membranes indicate that VP4 and the N terminus of VP1 together may form an "umbilicus" which tethers the virus to the endosomal membrane (46, 48).

Unlike enteroviruses, the aphthoviruses and cardioviruses do not produce stable empty capsids during uncoating *in vitro*. The aphthoviruses foot-and-mouth disease virus (FMDV) and equine rhinitis A virus (ERAV) disassemble into pentamers almost instantly after exposure to a pH critical for uncoating. Exposure to heat also induces disassembly. An uncoating intermediate/empty particle structure has been solved for ERAV from crystals grown at low pH (38). From this it was observed that VP4 is completely released from the capsid and the N terminus of VP2 may be externalized from the capsid, rather than VP1 as in enteroviruses. Due to this, it is hypothesized that the N terminus of VP2 will be involved in endosomal tethering in aphthoviruses (38). Similarly, cardioviruses also do not produce stable empty particles; for example, heating of Saffold virus 3 to 42°C for 5 min induces particle disassembly; however, exposure for 2 min induces a mixture of empty and A-particles (49). A low-resolution cryo-electron microscopy (cryo-EM) structure of the A-particles shows that the particles have expanded and have released VP4 and that there is an unconnected density leaving the particle that might be the VP1 N-terminal arm (49). To summarize, the capsid rearrangements that occur in VP4-containing picornaviruses involve capsid expansion, release of VP4, and externalization of the N terminus of either VP1 or VP2.

However, less is known about uncoating in VP0-containing picornaviruses. To date, AiV is the only VP0-containing picornavirus for which an empty capsid structure has been determined. Cryo-EM structures of mature and empty AiV capsids produced by heating revealed that in the empty particle the N termini of VP0 and VP1 become disordered; however, no proteins were observed to be released or externalized (50). This differs from what is known about VP4-containing picornaviruses, where VP4 is released and the N terminus of either VP2 or VP1 becomes externalized. It is difficult to envisage a model for membrane interactions in which capsid proteins are not externalized. For AiV, it was proposed that during uncoating, capsid proteins become externalized but slide back inside the capsid after genome release (50). However, whether this observation is biologically relevant remains to be resolved, as it seems unlikely that capsid proteins could easily be reinternalized if they are inserted within a membrane.

In this study, the mechanism of AiV uncoating is analyzed using purified virus particles and a VP0 peptide. Using chemical inhibition assays, capsid stability assays, and liposome assays with purified virus, we show that acidification is essential for AiV entry and that uncoating and membrane interactions are also dependent on low pH. Using peptides in liposome assays, we also show that the N terminus of AiV VP0 plays an equivalent role to that seen in the VP4 proteins of other picornaviruses. Sequence alignments suggest this function may be conserved between all kobuviruses.

RESULTS

AiV endocytosis is dependent on endosome acidification. AiV capsids, in common with those of many other picornaviruses, are destabilized by low pH (44), suggesting that endosomal acidification may be a trigger for AiV uncoating. To test if endosome acidification was required for AiV entry, the virus was grown in the presence of the endosome acidification inhibitor NH_4Cl at a range of nontoxic concentrations. In untreated cultures or those treated with low concentrations (2 mM) of NH_4Cl, virus infection resulted in complete cytopathic effect (CPE) at 20 h postinfection (hpi), with viral titers of 2×10^6 to 3×10^6 PFU/mL. In contrast, in cultures treated with NH_4Cl at concentrations of 10 mM and above, the addition of virus did not lead to visible CPE and AiV titers at 20 hpi were reduced by over 99% (Fig. 1A). A time-of-addition study was then carried out to determine at what point in the virus life cycle NH_4Cl was inhibitory. An inhibitory

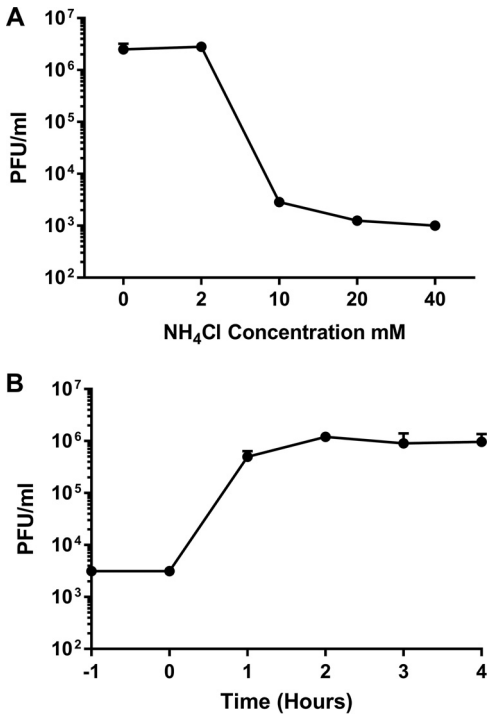

FIG 1 Inhibition of endosomal acidification interferes with an early step in the AiV life cycle. (A) Growth of AiV is prevented by treatment of cells with NH_4Cl. Titer of virus 24 h after infection of cells treated without, or with, 2 mM, 10 mM, 20 mM, or 40 mM NH_4Cl for 2 h before infection with AiV at an MOI of 1. (B) Time of addition of NH_4Cl shows effect early in infection. Titer of virus 24 h after infection of cells treated with 40 mM NH_4Cl 1 h before infection (−1) or 0, 1, 2, 3, or 4 h postinfection. Experiments were performed in triplicate.

concentration of NH_4Cl was added every hour to a different well of AiV-infected cells. This ranged from 1 h prior to infection to 4 h postinfection. This revealed that NH_4Cl was inhibitory only when added to cells prior to or during infection (Fig. 1B). When it was added 1 h postinfection, little reduction in titer was observed, and no reduction occurred when it was added 2 or more hours postinfection (Fig. 1B). This shows that NH_4Cl inhibits AiV infection during entry and not at another part of replication. This is consistent with the requirement for low pH for cell entry.

Decreasing pH enhances capsid alterations. Having shown that endosome acidification is important for AiV entry, we wanted to investigate the effect of pH on genome exposure and capsid protein dynamics. This was assessed using a particle stability thermal release assay (PaSTRy), which has previously been used to study uncoating dynamics and particle stability of enteroviruses, FMDV, and AiV (44, 51–54). To perform this, purified virus was incubated at a range of pH values with two dyes (SYTO9 and SYPRO orange). SYTO9 binds and fluoresces in the presence of nucleic acid, indicating genome accessibility. SYPRO orange binds and fluoresces in the presence of hydrophobic amino acid residues, indicating exposure of hydrophobic residues within the capsid proteins. During the assay, temperature was raised by 1°C every 30 s and the level of fluorescence of each dye was measured.

Previous studies with PaSTRy established that low pH can promote AiV genome exposure to occur at lower temperatures (44). Here, we have repeated this study using a finer range of pH values, between pH 7.0 and pH 4.9 (7.0, 6.2, 5.9, 5.6, 5.0, and 4.9), while also tracking the exposure of hydrophobic protein residues. Assays were performed after preincubating purified particles for 10 min at either room temperature, 56°C, or 59°C and then chilling them on ice for 2 min, prior to performing the assay.

With a room temperature preincubation, SYTO9 fluorescence began to be detectable between 48 and 49°C for pH 7.0, 6.2, and 5.9 with maximal fluorescence occurring

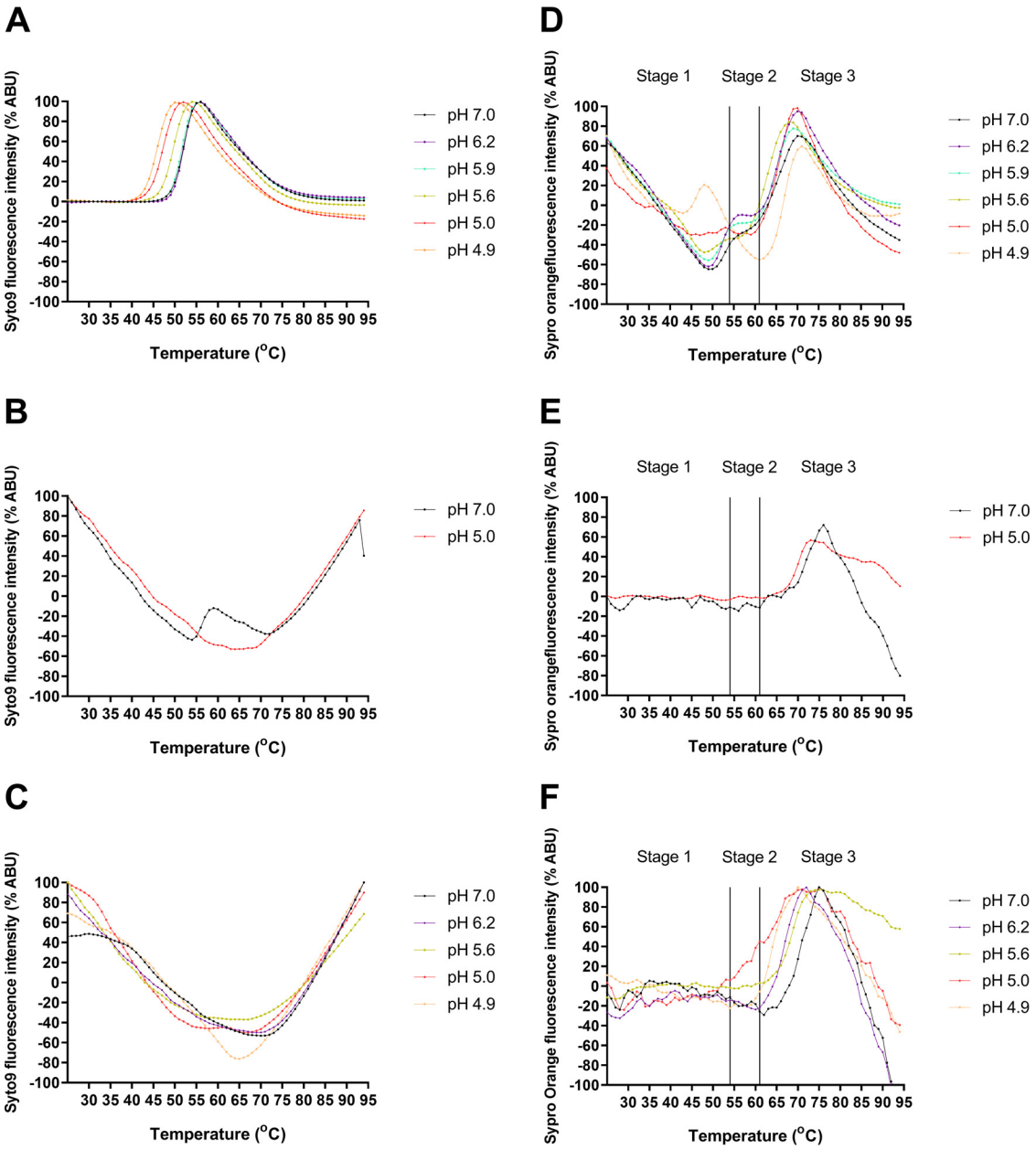

FIG 2 Low pH enhances AiV capsid alterations. AiV analyzed by PaSTRy over a range of pH values (pH 7.0, 6.2, 5.9, 5.6, 5.0, and 4.9) with incremental increases of temperature of 1°C every 30 s. Experiments were either put in at room temperature (A and D) or heated at either 56°C (B and E) or 59°C (C and F) for 10 min and then chilled on ice for 2 min prior to being put on the Stratagene MX3005p quantitative PCR (qPCR) system. (A to C) Relative fluorescence of SYTO9 nucleic acid-binding dye, where exposure is inferred from increasing signal of viral RNA. (D to F) Relative fluorescence of SYPRO orange hydrophobic protein residue-binding dye, where increasing signal infers exposure of hydrophobic capsid components. All results are normalized to maximum signal for each experiment, representing 100% signal. All experiments were performed in triplicate; this is a representative trace.

at 55°C. At pH 5.6 these values were reduced to 45 and 54°C, respectively. At pH 5 the fluorescence started at 42°C and peaked at 51°C, and at pH 4.9 these values were reduced to 41°C and 50°C, respectively (Fig. 2A). This showed that incubation at lower pH reduces the temperature for RNA exposure. When experiments were repeated with samples preincubated at 56°C, a greatly reduced peak signal was observed at pH 7.0 and no peak was observed at pH 5.0 (Fig. 2B). For samples preheated to 59°C, no SYTO9 peak was observed for samples (pH 7.0, 6.2, 5.6, 5.0, and 4.9) (Fig. 2C).

Therefore, overall, as pH decreased, the exposure of nucleic acid appeared to occur at lower temperatures. Results from the preincubation at 56°C indicate that low pH has

enhanced genome release and not just exposure, as a peak being present at pH 7.0 but not pH 5.0 indicates that at pH 7.0 some RNA remains within the capsid but that at pH 5.0 it has been completely released.

The effect that different pH values had on the profile of hydrophobic protein dynamics as measured by fluorescence is more complex. For simplicity we have separated the profiles into three stages based on events occurring at specific temperatures (Fig. 2D). Stage 1 (25 to 54°C) for samples preincubated at room temperature is characterized by a trough at pH 7.0, 6.2, 5.9, and 5.6; the trough becomes increasingly shallow at lower pH values. At pH 5.0 no trough was observed, and instead, the profile resembled a flat line; finally at pH 4.9 a peak was observed. The peak for the hydrophobic protein fluorescence at pH 4.9 occurred 2°C before the maximum peak of RNA exposure (Fig. 2B). Stage 2 (54 to 62°C) is characterized by a sloping shoulder at pH 7; at pH 6.2 and 5.9 the shoulder is flatter, at pH 5.6 and 5 it is almost indistinguishable from the trough in stage 1, and at pH 4.9 it has become a distinct trough. The beginning of stage 2 coincides with maximum RNA exposure for pH 7, 6.2, and 5.9. At stage 3 (62 to 95°C) a final large peak is observed under all conditions. The exact temperature at which the peak occurs and its magnitude vary between different pH values; this likely represents protein denaturation and is not physiologically relevant. Profiles of AiV at pH 4.9 resemble PaSTRy results previously observed for enteroviruses at neutral pH; however, AiV profiles differ when incubated between pH 7.0 and 5.0 (52, 53). When samples were preincubated at 56 or 59°C, a flat line was observed at stage 1 and stage 2 but the final stage 3 peak was still observed (Fig. 2E and F).

The experiments described here have shown that reductions in pH enhance genome release, alter capsid dynamics, and increase exposure of hydrophobic capsid residues at lower temperatures. The observation that the signals for exposure of genome and hydrophobic residues were reduced after preheating at elevated temperatures indicates that the changes that occur during heating are irreversible.

Membrane interactions and pore formation. Since it was established that pH plays an important role in AiV uncoating, the effect of pH on the ability of AiV to permeabilize model membranes was investigated.

Purified AiV was incubated at a range of pH values with liposomes containing carboxyfluorescein (CF) dye at 37°C. Fluorescent dye release was measured every minute for 1 h. This revealed that AiV induces membrane permeabilization in a pH-dependent manner, with the rate of dye release increasing at lower pH values (Fig. 3A). Dye release after 1 h ranged from 12% at pH 7 to 90% at pH 4.9 (Fig. 3B).

In addition to increasing the rate of dye release, pH was also observed to change the profile of dye release curves. At pH 7.0, 6.2, and 5.9, AiV dye release curves were seen as a slope increasing at a steady constant rate, with the slope gradient increasing at the lower pH values. At pH 5.6, 5.0, and 4.9, there was an initial steady slope of release, before an exponential phase of release occurring at 20, 15, and 10 min, respectively, before this leveled off (Fig. 3A). We have also investigated size selectivity using a dextran release assay. Samples of purified virus were incubated for 1 h at pH 7.0 or pH 5.0 in the presence of liposomes containing fluorescein isothiocyanate (FITC)-labeled dextran of different sizes (4 kDa [FD4], 10 kDa [FD10], 70 kDa [FD70], or 250 kDa [FD250]) (Fig. 3C and D). Release of dextrans was quantified by pelleting the liposomes and measuring the fluorescence in the supernatant. This revealed that AiV capsids preferentially released the two smallest dextrans (FD4 and FD10) and therefore appeared to form a size-selective pore, consistent with previous published results with RV16 (2). The predicted size of the pore is consistent with the size necessary to allow passage of unfolded single-stranded RNA (2). The effect of dye release for FD4 and FD10 was significantly higher at pH 5.0, giving further evidence that AiV-induced pore formation is enhanced by low pH.

We have previously shown that for another picornavirus in which cell entry is dependent on endosome acidification (RV16), the ability of the virus to permeabilize membranes was increased at lower pH values (2). In this previous study, the profile of RV16 dye release curves differed from AiV dye release curves in the current study. For

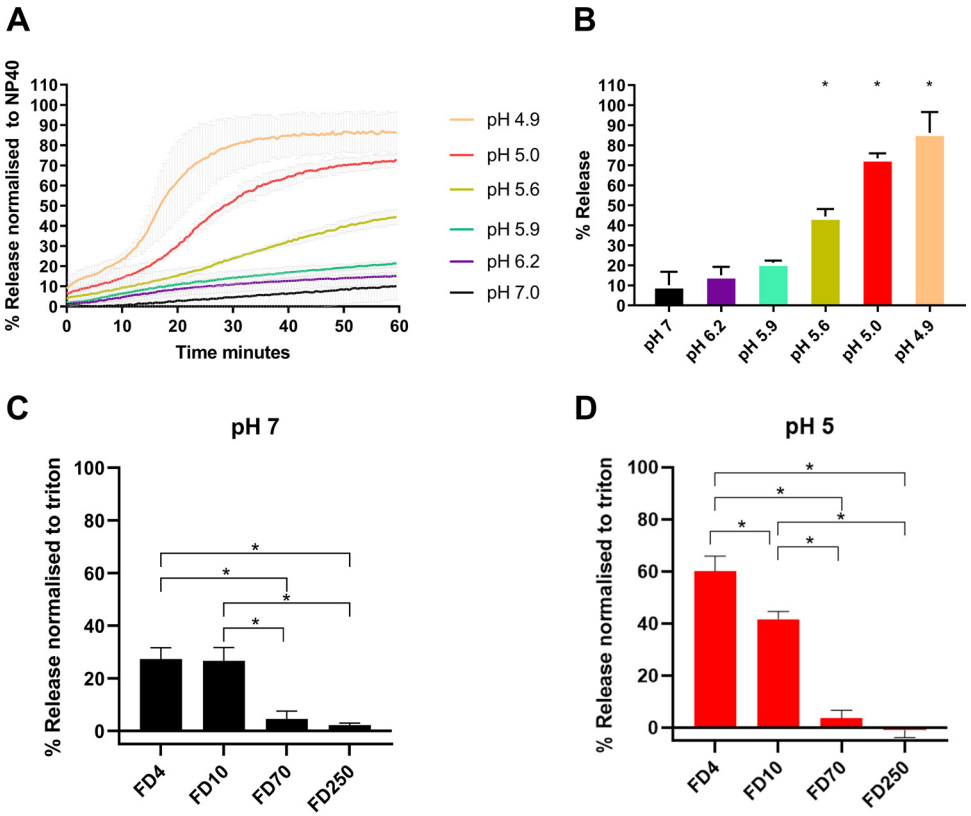

FIG 3 AiV-induced membrane permeability is enhanced by low pH. (A) Permeability assay showing CF released from liposomes after mixing with AiV at pH 7.0, 6.2, 5.9, 5.6, 5.0, and 4.9. CF was detected by fluorescence measurements (excitation, 492 nm/emission, 512 nm) recorded every 30 s for 1 h. (B) Endpoints of AiV-induced membrane permeability. Data in panel A were normalized to the maximum signal induced by 0.1% NP-40 at each pH value. (C and D) FD released after addition of 1 μg of purified AiV capsid liposomes containing FD of 4 kDa (FD4), 10 kDa (FD10), 70 kDa (FD70), or 250 kDa (FD250) at pH 7 (C) and pH 5 (D). Experiments were performed in triplicate, and error is measured by standard error of the mean (SEM). *, $P \geq 0.01$. Low pH is known to quench CF dye, so all results are normalized to 100% release as determined by incubation with NP-40 and 0% release as determined by liposome incubated alone. As low pH quenches CF/FITC fluorescence, the values were calculated as a percentage of full release by normalizing to untreated liposomes (0% release) and 0.1% NP-40 or Triton (100% release).

RV16 there was a high rate of dye release initially and the curve gradient gradually reduced over time; incubation at different pH values affected the rate of release, but the profile remained the same. This could represent differences in uncoating dynamics of AiV and RV16.

The role of VP0 in membrane permeability and pore formation in AiV. In other picornaviruses and picorna-like viruses, VP4 has been shown to be the component of the capsid that permeabilizes membranes (1–7). For RV16, VP4 forms a size-selective pore consistent with the size required for passage of single-stranded nucleic acid; specifically, the first 45 amino acids are able to induce pore formation (7). Also, residue 28 of PV has been shown to be involved with VP4 membrane permeability (5). In VP0 viruses such as AiV, which do not undergo VP0 cleavage to form VP4 and VP2, it is hypothesized the N terminus of VP0 will carry out this role. Given that the pore-forming part of the enterovirus VP4 appears to be present in the first 45 amino acids, we investigated if there was conservation between VP4 sequences across the picornavirus family and if this was shared by VP0 viruses. Alignment of VP4 from a variety of different genera was performed using MUSCLE (55). Alignments indicated a high degree of similarity of the amino acid properties of different picornavirus genera in the N terminus of VP4, especially in the region of amino acids 20 and 35 (Fig. 4A). This gives an indication that this region of VP4 may play a role in pore formation of all VP4

FIG 4 Alignments of VP4- and VP0-encoding picornavirus sequences. Alignments of picornavirus VP4 sequences (A) and VP0 sequences (B) were carried out using the MUSCLE sequence alignment tool (55). The amino acids are colored using the Zappo color scheme as follows: aliphatic/hydrophobic (pale pink), aromatic (orange), positively charged (purple), negatively charged (red), hydrophilic (green), conformationally special (magenta), and cysteine residues (yellow). Peptide sequence regions for AiV, LV, and RV are highlighted with a black box.

picornaviruses, consistent with this region containing the amino acid at position 28 mentioned earlier. We predict that this conserved motif is important for pore formation. We went on to look for conservation in VP0 viruses, comparing the first 109 amino acids of VP0 viruses from multiple genera using a MUSCLE alignment; this produced two groups of sequences which we refer to as "kobu-like" and "parecho-like." The alignment shows that parecho-like viruses lack strong conservation in this area and any other area of VP0. This is in contrast to kobu-like viruses, which have a high degree of conservation of amino acid properties in the first 20 amino acids of VP0 (Fig. 4B). Strong conservation can be indicative of an important and essential function. Therefore, this may suggest that the conserved VP4 motif in VP4 viruses and the conserved N terminus of VP0 in kobu-like viruses may have specific and essential functions. However, despite this conservation between VP4 sequences and between VP0 sequences, alignments between VP4 and VP0 did not show obvious similarities (data not shown). This suggests that there may be functional differences in how VP4 and VP0 interact with membranes.

To test if the N termini of VP0 from other picornaviruses were able to induce pore formation, CF liposome assays were carried out using peptides from representatives of both groups, using the first 50 amino acids of AiV VP0 (AiV-VP0-N50) and the parechovirus Ljungan virus (LV) VP0 (LV-VP0-N50) at pH 7. This revealed that AiV-VP0-N50 was

able to induce dye release in a dose-dependent manner, while LV-VP0-N50 was not (Fig. 5A and B). This is consistent with the VP0 sequence alignments where AiV and other kobu-like viruses show strong conservation in the N terminus of VP0, while LV and other parecho-like viruses lack strong conservation in this area (Fig. 4B and Fig. 5A and B). The peptides used here were not myristoylated, as it has previously been demonstrated that myristoylation is not essential for the replication of kobuviruses and parechoviruses (28).

Although the AiV peptide was able to induce membrane permeability, this appeared to be at a lower level than previously observed for RV16 peptides (7). To test if there was indeed a difference in permeabilization between RV16 and AiV peptides, we performed the assays with the peptides in parallel. This revealed that AiV-VP0-N50 was less effective at inducing membrane permeability than an unmyristoylated RV16-VP4-N45 (Fig. 5C).

As it has been established that AiV-VP0-N50 is able to permeabilize membranes, its ability to form a size-selective pore was compared with RV16 VP4 peptides, previously shown to form such a pore. To perform this, AiV-VP0-N50 and RV16-VP4-N45 peptides were incubated for 1 h at pH 7.0 in the presence of liposomes containing FITC-labeled dextrans of different sizes (4 kDa [FD4], 10 kDa [FD10], 70 kDa [FD70], or 250 kDa [FD250]) (Fig. 5D and E). Release of dextrans was quantified by pelleting the liposomes and measuring the fluorescence in the supernatant. This revealed that, like RV16 VP4 and AiV capsids, AiV VP0 preferentially releases the smallest dextran (FD4) and therefore forms a size-selective pore (2).

Next, the abilities of AiV-VP0-N50 to permeabilize membranes were compared between pH 7.0 and pH 5.0. This revealed that pH 5.0 enhanced dye release of the peptide (Fig. 5F). However, the dye release profiles at pH 5 differ between peptide and virus (Fig. 3A and Fig. 5F). For the virus, a sharp increase followed by leveling off was observed, but for the peptide, a constant gradual increase and no leveling were observed (Fig. 3A and Fig. 5C).

DISCUSSION

In this study, we sought to investigate uncoating and membrane interactions in the VP0-containing picornavirus AiV. This virus is of particular interest given the paucity of studies which have investigated uncoating in VP0-containing viruses. We have demonstrated that the N terminus of AiV VP0 is a pore-forming unit of the capsid, indicating that its function is likely analogous/similar to VP4 in VP4-containing picornaviruses. Also, using a combination of stability assays, membrane permeability assays, and chemical inhibition, we have demonstrated that pH plays a critical role in AiV uncoating and membrane interactions.

Here, we have shown AiV requires endosome acidification for entry, and using PaSTRy, we demonstrated that incubation of AiV at a pH of 5.6 and below enhances AiV genome exposure and alters the exposure of hydrophobic capsid proteins; this corresponds with the pH of late endosomes. The changes in PaSTRy profile were enhanced as pH was lowered even further, with a very dramatic shift occurring between pH 5.0 and 4.9. At present we are unable to explain this dramatic difference in profile when the pH differs by just 0.1. At pH 4.9, but no other pH, an increase in hydrophobic protein signal is detected a few degrees before nucleic acid signal is detected. These events are thought to represent genome release and the externalization of internal capsid proteins. After maximum nucleic acid signal is detected, there is a large drop in hydrophobic signal, causing a trough. This may indicate that during uncoating, internal capsid proteins are externalized and then reinternalized after genome release. This would be consistent with structural data on AiV empty particles produced by heating capsids at neutral pH, which reveal that VP1 and VP0 are inside the capsid after genome release, indicating they may be externalized during uncoating and become reinternalized after genome release (50). However, PaSTRys performed on particles preheated (so that genome release had already occurred) no longer showed this trough. This indicates the capsid rearrangements that occur during or after genome release are irreversible, and if proteins are reinternalized after genome release,

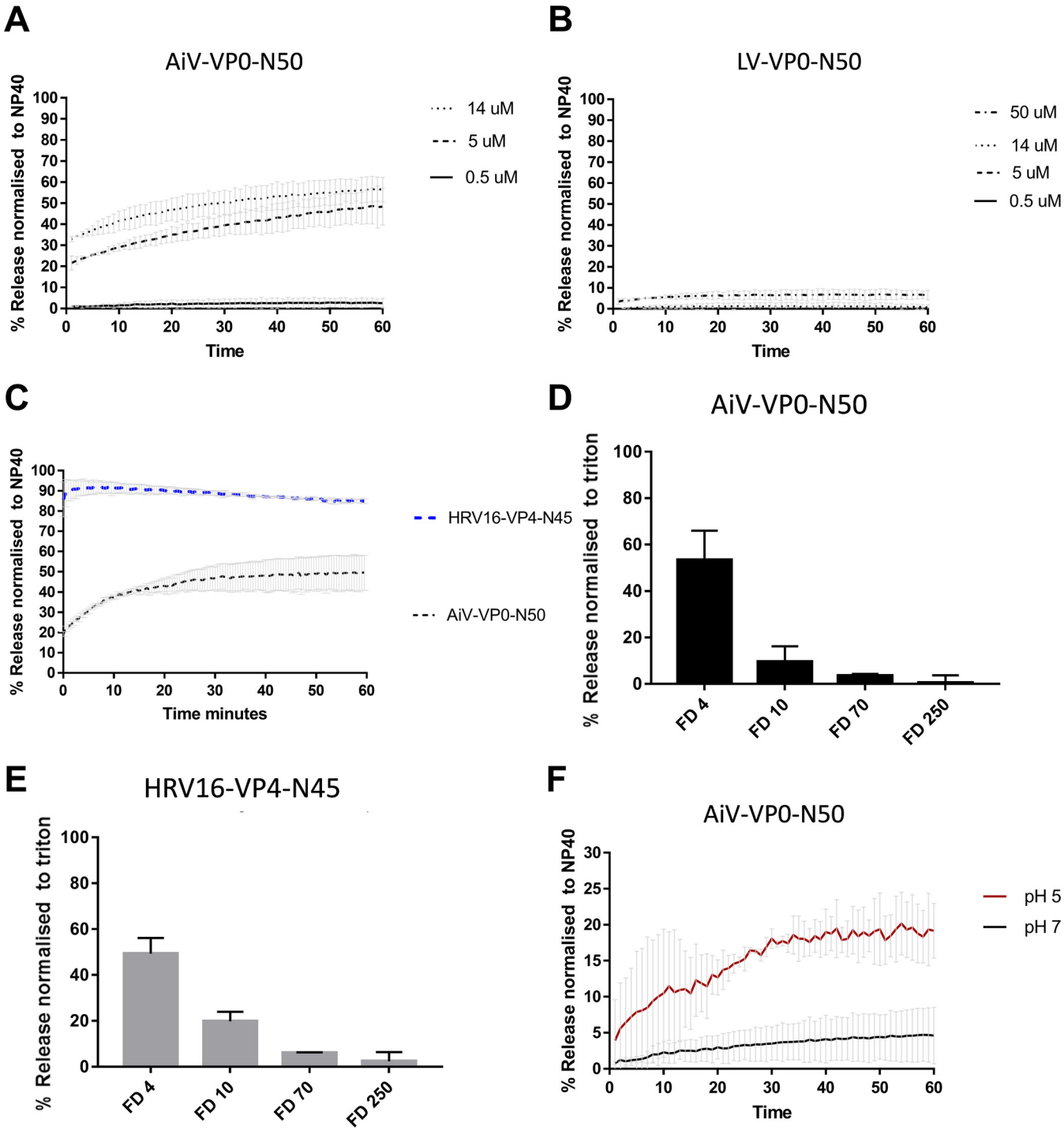

FIG 5 AiV VP0 N-terminal peptide is able to permeabilize membranes and form a size-selective pore. Permeability assays showing CF or fluorescent dextrans (FD) released from liposomes after mixing with peptides. CF or FD was detected by fluorescence measurements (excitation, 492 nm/emission, 512 nm) and displayed as percentage of total release by detergent-induced lysis. Assays were carried out at pH 7.0 unless otherwise stated. (A) CF release over time after addition of peptide AiV-VP0-N50 at concentrations of 0.5 μM, 5 μM, and 14 μM. (B) CF release over time after addition of peptide Ljungan virus (LV) LV-VP0-N50 at concentrations of 0.5 μM, 5 μM, 14 μM, and 50 μM. (C) CF release over time after addition of peptide AiV-VP0-N50 or RV16-VP4-N45 at concentrations of 5 μM. (D) FD released after addition of 5 μM peptide AiV-VP0-N50 to liposomes containing FD of 4 kDa (FD4), 10 kDa (FD10), 70 kDa (FD70), or 250 kDa (FD250). (E) FD released after addition of 5 μM peptide RV16-VP4-N45 to liposomes containing FD of 4 kDa (FD4), 10 kDa (FD10), 70 kDa (FD70), or 250 kDa (FD250). (F) CF release over time after addition of 0.5 μM peptide AiV-VP0-N50 at pH 5 or pH 7. All experiments were performed in triplicate, and error is measured by SEM. *, $P \geq 0.01$. As low pH quenches CF/FITC fluorescence, the values were calculated as a percentage of full release by normalizing to untreated liposomes (0% release) and 0.1% NP-40 or Triton (100% release). In FITC reactions pH of supernatant was neutralized by addition of a 2.5 M Tris (pH 7.5) buffer. Peptide sequences were as follows: AiV-VP0-50N, GNSVTNIYGNGNNVTTDVGANGWAPTVSTGLGDGPVSASADSLPGRSGGA; LV-VP0-50N, MAASKM NPVGNLLSTVSSTVGSLLQNPSVEEKEMDSDRVAASTTTNAGNL; RV16-VP4-45N, MGAQVSRQNVGTHSTQNMVSNGSSINYFNINYFKDAASSGASRLD.

their externalization can no longer be initiated by heating. Furthermore, the biological relevance/implications of this *in vitro* observation still remain to be addressed. If rearranged capsid proteins were inserted into a membrane first, it would likely be more difficult for them to be removed from the membrane and reinternalized into the capsid, as previous structural data (50), along with our biochemical data, suggest they do in the absence of membranes.

Whatever the biological relevance though, our PaSTRy results and previous structures highlight a difference *in vitro* between AiV and enterovirus uncoating. Enterovirus structures show that VP4 is completely released from the capsid and that the externalized termini of VP1 remain externalized after genome release (29, 35–37). Previously published data for enteroviruses with PaSTRy are consistent with this, with no apparent hydrophobic protein trough occurring after the nucleic acid peak (52, 53).

In addition to enhancing uncoating, incubation at a more acidic pH also enhances the ability of AiV to permeabilize model membranes. When AiV is incubated at pH 7.0, it induces relatively low levels of dye release; reducing the pH to 6.2 and 5.9 caused a moderate increase in dye release. In PaSTRys these pH values did not affect genome exposure and had similar hydrophobic protein profiles as pH 7.0. When the pH is lowered to 5.6 and below, the rate of AiV-induced dye release increases significantly before leveling off; this effect becomes more pronounced as the pH decreases further (Fig. 3). These significant increases in dye release coincide with PaSTRy profiles with enhanced hydrophobic signal. This suggests that externalization of hydrophobic capsid protein residues enhances AiV-induced membrane permeabilization; this is consistent with models of enterovirus-induced membrane permeabilization (45). The liposome assay profiles observed for AiV differ from what we have seen previously for the enterovirus RV16. For RV16, particles were able to induce dye release at neutral pH, and dye release was enhanced at low pH, but there was a gradual increase in the rate of release, rather than a sudden increase in release and then leveling off, which we observed for AiV (2). This may indicate that low pH plays a more critical role in AiV particle alterations and membrane interactions than for RV16.

Given that incubation of AiV at low pH increases the level of hydrophobic protein residues detected in PaSTRy and enhances membrane interactions, it is likely that low pH induces externalization of capsid components essential for AiV membrane interactions. It might therefore be expected that free peptide would induce higher levels of membrane permeability at physiological pH than virus. However, this was not observed: VP0-N-50 peptide at 0.5 μM induced smaller amounts of dye release than virus containing the equivalent of 0.1 μM VP0-N-50 at pH 7.0 and pH 5.0. As free peptide is less efficient at inducing membrane permeability than the virus, this indicates either that additional components of the capsid are also involved in membrane permeabilization or that VP0 N must be physically attached to the capsid to maintain its optimal pore-forming conformation. Low pH also enhances the ability of the VP0-N-50 peptide to form a pore; this is not surprising given that this would be the natural environment in which it would be required to form a pore. This is consistent with observations that the ability of RV16 VP4 protein to induce pore formation is enhanced at acidic pH (2).

Furthermore, using an N-terminal peptide of AiV VP0, we demonstrated VP0 forms a size-selective pore in model membranes consistent with a pore size able to release a molecule of single-stranded RNA. This demonstrates the N terminus of AiV VP0 plays an analogous function to VP4 of other picornaviruses in terms of membrane permeabilization (1–6). However, the N terminus of VP0 does not appear to be the pore-forming component of all VP0-containing picornaviruses, as an N-terminal peptide for LV did not induce dye release from liposomes.

Sequence comparison of VP0 N termini revealed that the VP0 N termini of AiV and other kobu-like VP0 viruses are well conserved; this suggests that the N terminus of VP0 likely plays a pore-forming role for all kobu-like VP0 viruses. Similar levels of homology are seen between VP4 sequences in other picornavirus genera. However, comparison of LV and other parecho-like VP0 viruses revealed that VP0 N termini are

not well conserved; this would be consistent with them not being involved in membrane interactions in these viruses. Taken together, this seems to indicate that the N terminus of the VP0 of viruses in kobu-like viruses possesses the ability to form a pore, while the parecho-like group lacks N-terminal membrane permeabilization activity.

The ability of other AiV proteins to interact with membranes is yet to be determined. For enteroviruses, it has been demonstrated that the N terminus of VP1 is essential for attachment to model membranes in flotation assays. The N terminus of VP1 is internal in native particles and is released during conversion to A-particles. It was shown that in flotation assays, A-particles bound to model membranes, while native particles and A-particles where the VP1 N terminus had been cleaved by proteolytic digestion were unable to bind model membranes (30). Furthermore, when A-particles bound to model membranes were subjected to proteolytic digestion, the N terminus of VP1 remained within the membranes (30), further demonstrating that VP1 is required for membrane attachment in enteroviruses (30). If consistent with enteroviruses, the AiV N terminus of VP1 will become externalized and be involved in attachment to the endosomal membrane. However, unlike in VP4-containing picornaviruses, AiV VP0 remains attached to the capsid, so it is possible that it may play an important role in attachment alongside or instead of VP1.

Conclusion. This study is the first to characterize effects of pH on the uncoating and membrane interactions of a VP0-containing picornavirus. We have shown that the N terminus of VP0 can play a role in pore formation but not in all VP0-containing picornaviruses. We have also demonstrated that AiV behaves differently in functional uncoating assays compared to enteroviruses. Together with previous structural studies, this indicates that AiV capsids likely undergo different structural changes in the capsid to initiate membrane interactions and uncoating than VP4-containing picornaviruses. AiV also appears to have a greater dependence on pH to facilitate externalization of membrane-interacting components than enteroviruses. Further characterization will be required to determine the exact uncoating mechanism of AiV.

MATERIALS AND METHODS

Cell lines and virus. Vero cells were obtained from the Central Services Unit at The Pirbright Institute and propagated in Dulbecco modified Eagle medium (DMEM) containing 10% fetal bovine serum (FBS) and 50 μg/mL penicillin and streptomycin at 37°C in a humidified atmosphere containing 5% CO_2. AiV strain A846/88 (GenBank no. BAA31356.1) was obtained from David Stuart and Elizabeth Fry at the University of Oxford. Virus was propagated by inoculating Vero cells at a multiplicity of infection (MOI) of 1 and incubating them at 37°C in a humidified atmosphere containing 5% CO_2 for 24 h before the supernatant was harvested.

Peptides. Peptides were synthesized by Peptide Protein Research Ltd. using the Peptide Synthetics service. The sequences were as follows: AiV-VP0-50N, GNSVTNIYGNGNNVTTDVGANGWAPTVSTGLG DGPVSASADSLPGRSGGA; LV-VP0-50N, MAASKMNPVGNLLSTVSSTVGSLLQNPSVEEKEMDSDRVAASTTTNAG NL; RV16-VP4-45N, MGAQVSRQNVGTHSTQNMVSNGSSINYFNINYFKDAASSGASRLD.

Chemical inhibition. Vero cells were seeded into a 6-well plate at 3×10^5 cells in 2 mL of 10% FBS-DMEM per well and incubated at 37°C overnight. Medium was removed from the wells, and the cells were pretreated with medium containing NH_4Cl (ammonium chloride) (Sigma-Aldrich) (2, 10, 20, 40 mM), for 2 h at 37°C. Cells were then incubated on ice with virus to allow attachment (MOI = 1) for 30 min in the presence of inhibitor. Unbound virus was removed, and cells were washed with phosphate-buffered saline (PBS), before adding 2 mL of warm serum-free DMEM containing inhibitor to the wells. For time-of-addition studies, cells were infected with AiV at an MOI of 1 and medium was replaced with 40 mM NH_4Cl at 0, 1, 2, 3, or 4 h postinfection. After incubation overnight at 37°C for 20 h, the supernatants were harvested and the virus titers were determined by plaque assay.

Plaque assay. Six-well plates were seeded with 3×10^5 Vero cells per well. The following day AiV samples to be titrated were serially diluted in serum-containing medium. Medium was removed from wells, and 200 μL of each serial dilution was added to individual wells and incubated for 2 h. After 2 h, supernatant was removed and 2 mL of serum-containing medium with 1% agarose at 42°C was added to each well and allowed to solidify. Plates were incubated at 37°C in a humidified atmosphere containing 5% CO_2 for 72 h. Monolayers were fixed and stained with 1 mL of 4% formaldehyde, 1% crystal violet, 20% ethanol in PBS; plaques were counted; and titer was expressed as PFU/mL of starting material.

Purification of virus. Infected cell cultures were lysed by addition of NP-40 to make the solution a final concentration of 0.5% NP-40 and freeze-thawing three times. Lysates were incubated for 3 h at 37°C in the presence of DNase (10 μM) and clarified by centrifugation. Clarified supernatants were concentrated by precipitation with 8% polyethylene glycol (PEG) 8000 overnight and centrifugation at 100,000 relative centrifugal force (RCF) for 1 h. The resulting pellet was resuspended in PBS, pelleted

through a 2-mL cushion of 30% (wt/vol) sucrose in PBS at 125,755 RCF for 2 h, resuspended in PBS, and subjected to sedimentation in a sucrose density gradient comprising 15 to 45% (wt/vol) sucrose in PBS at 237,000 RCF for 50 min. Sucrose gradients were fractionated, and purified virus was quantified by absorbance at 260 nm. Sucrose was removed using a Zeba column (ThermoFisher Scientific) following the manufacturer's instructions.

Particle stability thermal release assay (PaSTRy). Virus particle alterations were characterized by a thermofluorometric dual dye-binding assay using the nucleic acid dye SYTO9 and the protein-binding dye SYPRO orange (both from Invitrogen). Reaction mixtures of 50 μL containing 1.0 μg of purified virus and 0.1 M citric acid-0.2 M sodium phosphate dibasic buffer at either pH 7, 6.2, 5.9, 5.6, 5.0, or 4.9 were mixed and incubated at either room temperature, 56°C, or 59°C for 10 min and then chilled on ice for 2 min. Reaction mixes were then made to 5 μM SYTO9 and 150$\times$ SYPRO orange and ramped from 25 to 95°C, with fluorescence reads taken at 1°C intervals every 30 s within the Stratagene MX3005p quantitative PCR (qPCR) system.

Preparation of liposomes. Liposomes comprising phosphatidic acid, phosphatidylcholine, cholesterol, and rhodamine-labeled phosphatidylethanolamine (Avanti Polar Lipids) (molar ratios 44.5:44.5:10:1, respectively) were prepared as previously described (6) by rehydration of dried lipid films in 107 mM NaCl, 10 mM HEPES, pH 7.5, and extrusion through 400-nm-pore-size membranes using a miniextruder (Avanti Polar Lipids). The lipid concentration of liposome preparations was estimated by measuring the level of rhodamine fluorescence in the liposome sample relative to samples of rehydrated lipids of known concentration. The expected diameter (average, 400 nm) and size distribution of liposomes were confirmed by dynamic light scattering (Malvern Zetasizer μV). Liposomes containing carboxyfluorescein (CF) (Sigma) were prepared by rehydrating lipids in the presence of 50 mM CF, 10 mM HEPES, pH 7.5. Liposomes containing FITC-conjugated dextrans (FD; Sigma) were prepared by rehydrating lipids in the presence of 25 mg/mL FD, 107 mM NaCl, 10 mM HEPES, pH 7.5. Liposomes containing CF or FD were purified from external fluorescence by multiple cycles of ultracentrifugation (1) and resuspended in 107 mM NaCl, 10 mM HEPES, pH 7.0, or 0.1 M citric acid, 0.2 M sodium phosphate, pH 7, 6.2, 5.9, 5.6, 5.0, or 4.9.

Membrane permeability assays. Membrane permeability was measured by detecting the release of fluorescent material from within liposomes. Purified liposomes containing CF or FD were added to test substances (peptide, virus, or mock controls in a typical volume of 5 μL) to give typical final concentrations of 50 μM lipid, 107 mM NaCl, 10 mM HEPES, pH 7.4, or 0.1 M citric acid, 0.2 M sodium phosphate, pH 7.0, 6.2, 5.9, 5.6, 5.0, or 4.9, and total volume of 100 μL. Reagents and plasticware were preequilibrated to the reaction temperature (25°C or 37°C).

For CF release, reaction mixtures were assembled in 96-well plates and membrane permeability was detected in real time by the release, dequenching, and increase in fluorescence of CF. Measurements were recorded every 30 s for 1 h using a fluorescence plate reader with excitation and emission wavelengths of 485 nm and 520 nm, respectively (Plate Chameleon V; Hidex). Initial rates were calculated from the linear slope of lines generated from the initial four data points.

For experiments investigating the effect of pH on the induction of membrane permeability, CF release reaction mixtures were assembled with 0.1 M citric acid, 0.2 M sodium phosphate, pH 7.0, 6.2, 5.9, 5.6, or 5.0 (instead of HEPES). As low pH quenches CF fluorescence, the values were calculated as a percentage of full release by normalizing to untreated liposomes (0% release) and 0.1% NP-40 (100% release).

FD release reaction mixtures were assembled with 10 mM citric acid and 10 mM sodium phosphate at pH 5 and pH 7. Reaction mixtures were incubated for 1 h, liposomes were pelleted at 100,000 $\times$ *g* for 30 min, and pH of supernatant was neutralized by addition of a 2.5 M Tris (pH 7.5) buffer. Fluorescent signal in the supernatant was measured using the plate reader as described above. The pelleted liposome signal was then released by the addition of Triton to calculate a 100% release signal.

ACKNOWLEDGMENTS

We thank David Stuart and Elizabeth Fry at the University of Oxford for the kind gift of AiV.

REFERENCES

1. Davis MP, Bottley G, Beales LP, Killington RA, Rowlands DJ, Tuthill TJ. 2008. Recombinant VP4 of human rhinovirus induces permeability in model membranes. J Virol 82:4169–4174. https://doi.org/10.1128/JVI.01070-07.
2. Panjwani A, Strauss M, Gold S, Wenham H, Jackson T, Chou JJ, Rowlands DJ, Stonehouse NJ, Hogle JM, Tuthill TJ. 2014. Capsid protein VP4 of human rhinovirus induces membrane permeability by the formation of a size-selective multimeric pore. PLoS Pathog 10:e1004294. https://doi.org/10.1371/journal.ppat.1004294.
3. Shukla A, Padhi AK, Gomes J, Banerjee M. 2014. The VP4 peptide of hepatitis A virus ruptures membranes through formation of discrete pores. J Virol 88:12409–12421. https://doi.org/10.1128/JVI.01896-14.
4. Sánchez-Eugenia R, Goikolea J, Gil-Cartón D, Sánchez-Magraner L, Guérin DMA. 2015. Triatoma virus recombinant VP4 protein induces membrane permeability through dynamic pores. J Virol 89:4645–4654. https://doi.org/10.1128/JVI.00011-15.
5. Danthi P, Tosteson M, Li Q-H, Chow M. 2003. Genome delivery and ion channel properties are altered in VP4 mutants of poliovirus. J Virol 77:5266–5274. https://doi.org/10.1128/jvi.77.9.5266-5274.2003.
6. Tuthill TJ, Bubeck D, Rowlands DJ, Hogle JM. 2006. Characterization of early steps in the poliovirus infection process: receptor-decorated liposomes induce conversion of the virus to membrane-anchored entry-intermediate particles. J Virol 80:172–180. https://doi.org/10.1128/JVI.80.1.172-180.2006.
7. Panjwani A, Asfor AS, Tuthill TJ. 2016. The conserved N-terminus of human rhinovirus capsid protein VP4 contains membrane pore-forming activity and is a target for neutralizing antibodies. J Gen Virol 97:3238–3242. https://doi.org/10.1099/jgv.0.000629.

8. Rossmann MG, Arnold E, Erickson JW, Frankenberger EA, Griffith JP, Hecht HJ, Johnson JE, Kamer G, Luo M, Mosser AG. 1985. Structure of a human common cold virus and functional relationship to other picornaviruses. Nature 317:145–153. https://doi.org/10.1038/317145a0.
9. Arnold E, Luo M, Vriend G, Rossmann MG, Palmenberg AC, Parks GD, Nicklin MJ, Wimmer E. 1987. Implications of the picornavirus capsid structure for polyprotein processing. Proc Natl Acad Sci U S A 84:21–25. https://doi.org/10.1073/pnas.84.1.21.
10. Hogle JM, Chow M, Filman DJ. 1985. Three-dimensional structure of poliovirus at 2.9 A resolution. Science 229:1358–1365. https://doi.org/10.1126/science.2994218.
11. Zhang Q, Hu R, Tang X, Wu C, He Q, Zhao Z, Chen H, Wu B. 2013. Occurrence and investigation of enteric viral infections in pigs with diarrhea in China. Arch Virol 158:1631–1636. https://doi.org/10.1007/s00705-013-1659-x.
12. Yamashita T, Ito M, Kabashima Y, Tsuzuki H, Fujiura A, Sakae K. 2003. Isolation and characterization of a new species of kobuvirus associated with cattle. J Gen Virol 84:3069–3077. https://doi.org/10.1099/vir.0.19266-0.
13. Carmona-Vicente N, Buesa J, Brown PA, Merga JY, Darby AC, Stavisky J, Sadler L, Gaskell RM, Dawson S, Radford AD. 2013. Phylogeny and prevalence of kobuviruses in dogs and cats in the UK. Vet Microbiol 164:246–252. https://doi.org/10.1016/j.vetmic.2013.02.014.
14. Bergallo M, Galliano I, Montanari P, Rassu M, Daprà V. 2017. Aichivirus in children with diarrhea in northern Italy. Intervirology 60:196–200. https://doi.org/10.1159/000487051.
15. Sdiri-Loulizi K, Hassine M, Bour JB, Ambert-Balay K, Mastouri M, Aho LS, Gharbi-Khelifi H, Aouni Z, Sakly N, Chouchane S, Neji-Guédiche M, Pothier P, Aouni M. 2010. Aichi virus IgG seroprevalence in Tunisia parallels genomic detection and clinical presentation in children with gastroenteritis. Clin Vaccine Immunol 17:1111–1116. https://doi.org/10.1128/CVI.00059-10.
16. Yamashita T, Sakae K, Ishihara Y, Isomura S, Utagawa E. 1993. Prevalence of newly isolated, cytopathic small round virus (Aichi strain) in Japan. J Clin Microbiol 31:2938–2943. https://doi.org/10.1128/jcm.31.11.2938-2943.1993.
17. Oh D-Y, Silva PA, Hauroeder B, Diedrich S, Cardoso DDP, Schreier E. 2006. Molecular characterization of the first Aichi viruses isolated in Europe and in South America. Arch Virol 151:1199–1206. https://doi.org/10.1007/s00705-005-0706-7.
18. Reuter G, Boros A, Pankovics P. 2011. Kobuviruses - a comprehensive review. Rev Med Virol 21:32–41. https://doi.org/10.1002/rmv.677.
19. Rivadulla E, Romalde JL. 2020. A comprehensive review on human Aichi virus. Virol Sin 35:501–516. https://doi.org/10.1007/s12250-020-00222-5.
20. Kitajima M, Gerba C. 2015. Aichi virus 1: environmental occurrence and behavior. Pathogens 4:256–268. https://doi.org/10.3390/pathogens4020256.
21. Tuthill TJ, Groppelli E, Hogle JM, Rowlands DJ. 2010. Picornaviruses. Curr Top Microbiol Immunol 343:43–89. https://doi.org/10.1007/82_2010_37.
22. Stanway G, Kalkkinen N, Roivainen M, Ghazi F, Khan M, Smyth M, Meurman O, Hyypiä T. 1994. Molecular and biological characteristics of echovirus 22, a representative of a new picornavirus group. J Virol 68:8232–8238. https://doi.org/10.1128/JVI.68.12.8232-8238.1994.
23. Yamashita T, Kobayashi S, Sakae K, Nakata S, Chiba S, Ishihara Y, Isomura S. 1991. Isolation of cytopathic small round viruses with BS-C-1 cells from patients with gastroenteritis. J Infect Dis 164:954–957. https://doi.org/10.1093/infdis/164.5.954.
24. Ansardi DC, Porter DC, Morrow CD. 1992. Myristylation of poliovirus capsid precursor P1 is required for assembly of subviral particles. J Virol 66:4556–4563. https://doi.org/10.1128/JVI.66.7.4556-4563.1992.
25. Marc D, Drugeon G, Haenni AL, Girard M, van der Werf S. 1989. Role of myristoylation of poliovirus capsid protein VP4 as determined by site-directed mutagenesis of its N-terminal sequence. EMBO J 8:2661–2668. https://doi.org/10.1002/j.1460-2075.1989.tb08406.x.
26. Goodwin S, Tuthill TJ, Arias A, Killington RA, Rowlands DJ. 2009. Foot-and-mouth disease virus assembly: processing of recombinant capsid precursor by exogenous protease induces self-assembly of pentamers in vitro in a myristoylation-dependent manner. J Virol 83:11275–11282. https://doi.org/10.1128/JVI.01263-09.
27. Mousnier A, Bell AS, Swieboda DP, Morales-Sanfrutos J, Perez-Dorado I, Brannigan JA, Newman J, Ritzefeld M, Hutton JA, Guedan A, Asfor AS, Robinson SW, Hopkins-Navratilova I, Wilkinson AJ, Johnston SL, Leatherbarrow RJ, Tuthill TJ, Solari R, Tate EW. 2018. Fragment-derived inhibitors of human N-myristoyltransferase block capsid assembly and replication of the common cold virus. Nat Chem 10:599–606. https://doi.org/10.1038/s41557-018-0039-2.
28. Corbic Ramljak I, Stanger J, Real-Hohn A, Dreier D, Wimmer L, Redlberger-Fritz M, Fischl W, Klingel K, Mihovilovic MD, Blaas D, Kowalski H. 2018. Cellular N-myristoyltransferases play a crucial picornavirus genus-specific role in viral assembly, virion maturation, and infectivity. PLoS Pathog 14:e1007203. https://doi.org/10.1371/journal.ppat.1007203.
29. Wang X, Peng W, Ren J, Hu Z, Xu J, Lou Z, Li X, Yin W, Shen X, Porta C, Walter TS, Evans G, Axford D, Owen R, Rowlands DJ, Wang J, Stuart DI, Fry EE, Rao Z. 2012. A sensor-adaptor mechanism for enterovirus uncoating from structures of EV71. Nat Struct Mol Biol 19:424–429. https://doi.org/10.1038/nsmb.2255.
30. Fricks CE, Hogle JM. 1990. Cell-induced conformational change in poliovirus: externalization of the amino terminus of VP1 is responsible for liposome binding. J Virol 64:1934–1945. https://doi.org/10.1128/JVI.64.5.1934-1945.1990.
31. Bostina M, Levy H, Filman DJ, Hogle JM. 2011. Poliovirus RNA is released from the capsid near a twofold symmetry axis. J Virol 85:776–783. https://doi.org/10.1128/JVI.00531-10.
32. Shingler KL, Yoder JL, Carnegie MS, Ashley RE, Makhov AM, Conway JF, Hafenstein S. 2013. The enterovirus 71 A-particle forms a gateway to allow genome release: a cryoEM study of picornavirus uncoating. PLoS Pathog 9:e1003240. https://doi.org/10.1371/journal.ppat.1003240.
33. Levy HC, Bostina M, Filman DJ, Hogle JM. 2010. Catching a virus in the act of RNA release: a novel poliovirus uncoating intermediate characterized by cryo-electron microscopy. J Virol 84:4426–4441. https://doi.org/10.1128/JVI.02393-09.
34. Ren J, Wang X, Hu Z, Gao Q, Sun Y, Li X, Porta C, Walter TS, Gilbert RJ, Zhao Y, Axford D, Williams M, McAuley K, Rowlands DJ, Yin W, Wang J, Stuart DI, Rao Z, Fry EE. 2013. Picornavirus uncoating intermediate captured in atomic detail. Nat Commun 4:1929. https://doi.org/10.1038/ncomms2889.
35. Seitsonen JJT, Shakeel S, Susi P, Arun P, Sinkovits RS, Hyvönen H, Ylä-Pelto J, Topf M, Hyypiä T, Butcher SJ, Pandurangan AP, Laurinmäki P. 2012. Structural analysis of coxsackievirus A7 reveals conformational changes associated with uncoating. J Virol 86:7207–7215. https://doi.org/10.1128/JVI.06425-11.
36. Garriga D, Pickl-Herk A, Luque D, Wruss J, Castón JR, Blaas D, Verdaguer N. 2012. Insights into minor group rhinovirus uncoating: the X-ray structure of the HRV2 empty capsid. PLoS Pathog 8:e1002473. https://doi.org/10.1371/journal.ppat.1002473.
37. Lyu K, Ding J, Han J-F, Zhang Y, Wu X-Y, He Y-L, Qin C-F, Chen R. 2014. Human enterovirus 71 uncoating captured at atomic resolution. J Virol 88:3114–3126. https://doi.org/10.1128/JVI.03029-13.
38. Tuthill TJ, Harlos K, Walter TS, Knowles NJ, Groppelli E, David J, Stuart DI, Fry EE. 2009. Equine rhinitis A virus and its low pH empty particle: clues towards an aphthovirus entry mechanism? PLoS Pathog 5:e1000620. https://doi.org/10.1371/journal.ppat.1000620.
39. Malik N, Kotecha A, Gold S, Asfor A, Ren J, Huiskonen JT, Tuthill TJ, Fry EE, Stuart DI. 2017. Structures of foot and mouth disease virus pentamers: insight into capsid dissociation and unexpected pentamer reassociation. PLoS Pathog 13:e1006607. https://doi.org/10.1371/journal.ppat.1006607.
40. Groppelli E, Tuthill TJ, Rowlands DJ. 2010. Cell entry of the aphthovirus equine rhinitis A virus is dependent on endosome acidification. J Virol 84:6235–6240. https://doi.org/10.1128/JVI.02375-09.
41. Nurani G, Lindqvist B, Casasnovas JM. 2003. Receptor priming of major group human rhinoviruses for uncoating and entry at mild low-pH environments. J Virol 77:11985–11991. https://doi.org/10.1128/jvi.77.22.11985-11991.2003.
42. Newman JF, Rowlands DJ, Brown F. 1973. A physico-chemical sub-grouping of the mammalian picornaviruses. J Gen Virol 18:171–180. https://doi.org/10.1099/0022-1317-18-2-171.
43. Curry S, Abrams CC, Fry E, Crowther JC, Belsham GJ, Stuart DI, King AM. 1995. Viral RNA modulates the acid sensitivity of foot-and-mouth disease virus capsids. J Virol 69:430–438. https://doi.org/10.1128/JVI.69.1.430-438.1995.
44. Zhu L, Wang X, Ren J, Kotecha A, Walter TS, Yuan S, Yamashita T, Tuthill TJ, Fry EE, Rao Z, Stuart DI. 2016. Structure of human Aichi virus and implications for receptor binding. Nat Microbiol 1:16150. https://doi.org/10.1038/nmicrobiol.2016.150.
45. Katpally U, Fu T-M, Freed DC, Casimiro DR, Smith TJ. 2009. Antibodies to the buried N terminus of rhinovirus VP4 exhibit cross-serotypic neutralization. J Virol 83:7040–7048. https://doi.org/10.1128/JVI.00557-09.
46. Strauss M, Levy HC, Bostina M, Filman DJ, Hogle JM. 2013. RNA transfer from poliovirus 135S particles across membranes is mediated by long umbilical connectors. J Virol 87:3903–3914. https://doi.org/10.1128/JVI.03209-12.

47. Li Q, Yafal AG, Lee YM, Hogle J, Chow M. 1994. Poliovirus neutralization by antibodies to internal epitopes of VP4 and VP1 results from reversible exposure of these sequences at physiological temperature. J Virol 68:3965–3970. https://doi.org/10.1128/JVI.68.6.3965-3970.1994.
48. Groppelli E, Levy HC, Sun E, Strauss M, Nicol C, Gold S, Zhuang X, Tuthill TJ, Hogle JM, Rowlands DJ. 2017. Picornavirus RNA is protected from cleavage by ribonuclease during virion uncoating and transfer across cellular and model membranes. PLoS Pathog 13:e1006197. https://doi.org/10.1371/journal.ppat.1006197.
49. Mullapudi E, Nováček J, Pálková L, Kulich P, Lindberg AM, van Kuppeveld FJM, Plevka P. 2016. Structure and genome release mechanism of the human cardiovirus Saffold virus 3. J Virol 90:7628–7639. https://doi.org/10.1128/JVI.00746-16.
50. Sabin C, Füzik T, Škubník K, Pálková L, Lindberg AM, Plevka P. 2016. Structure of Aichi virus 1 and its empty particle: clues towards kobuvirus genome release mechanism. J Virol 90:10800–10810. https://doi.org/10.1128/JVI.01601-16.
51. De Colibus L, Wang X, Spyrou JAB, Kelly J, Ren J, Grimes J, Puerstinger G, Stonehouse N, Walter TS, Hu Z, Wang J, Li X, Peng W, Rowlands DJ, Fry EE, Rao Z, Stuart DI. 2014. More-powerful virus inhibitors from structure-based analysis of HEV71 capsid-binding molecules. Nat Struct Mol Biol 21:282–288. https://doi.org/10.1038/nsmb.2769.
52. Walter TS, Ren J, Tuthill TJ, Rowlands DJ, Stuart DI, Fry EE. 2012. A plate-based high-throughput assay for virus stability and vaccine formulation. J Virol Methods 185:166–170. https://doi.org/10.1016/j.jviromet.2012.06.014.
53. Adeyemi OO, Nicol C, Stonehouse NJ, Rowlands DJ. 2017. Increasing type 1 poliovirus capsid stability by thermal selection. J Virol 91:e01586-16. https://doi.org/10.1128/JVI.01586-16.
54. Kotecha A, Zhang F, Juleff N, Jackson T, Perez E, Stuart D, Fry E, Charleston B, Seago J. 2016. Application of the thermofluor PaSTRy technique for improving foot-and-mouth disease virus vaccine formulation. J Gen Virol 97:1557–1565. https://doi.org/10.1099/jgv.0.000462.
55. Edgar RC. 2004. MUSCLE: multiple sequence alignment with high accuracy and high throughput. Nucleic Acids Res 32:1792–1797. https://doi.org/10.1093/nar/gkh340.